

Submitted: October 11, 2012

United States Nuclear Regulatory Commission Official Hearing Exhibit	
In the Matter of:	Entergy Nuclear Operations, Inc. (Indian Point Nuclear Generating Units 2 and 3)
	ASLBP #: 07-858-03-LR-BD01
	Docket #: 05000247   05000286
	Exhibit #: RIV000129-00-BD01
	Admitted: 10/15/2012
	Rejected:
Other:	Identified: 10/15/2012 Withdrawn: Stricken:

**G. J. Bignold, BSc, PhD, K. Garbett, BSc, PhD, R. Garnsey, BSc, PhD, C.Chem, FRSC, and I. S. Woolsey, BSc, PhD, CEGB, Leatherhead**

Erosion-corrosion of carbon steels has been experienced in the steam generator and secondary water circuits of many reactor systems. Damage has occurred under both single and two-phase water flow conditions, and is associated with severe fluid turbulence at the metal surface. In the most severe cases, this can lead to very high metal wastage rates (>1mm/year), and consequently rapid component failure. The available experience, previous research and current understanding of the phenomenon are reviewed, and both experimental and theoretical work in progress at CERL is described. The pH dependence of the phenomenon under single phase conditions at 148°C is reported, and by using hydrodynamically well characterized specimens, the dependence of erosion-corrosion rate on mass-transfer has been investigated. At 148°C, the rate has been found to vary as the cube of the mass transfer coefficient. This is in agreement with the predictions of a model of the process based on the electrochemical dissolution of magnetite. In order to make quantitative measurements on the process, high precision bore metrology and surface activation of the test specimens has been used extensively, and these measurement techniques are also discussed.

#### INTRODUCTION

1. Nuclear steam generators have experienced a wide variety of corrosion related problems, and the vulnerability of individual designs to any particular type of corrosion damage can vary widely. In all cases, however, the economic penalties resulting from such damage are considerable, and there is therefore a strong incentive to eliminate such problems as far as possible. To this end, a wide variety of research programmes are in progress throughout the world.

2. In many nuclear systems, corrosion has resulted from the generation of aggressive solutions via solute concentration processes (ref.1). This is particularly true in the case of PWR steam generators, for example with the denting, phosphate thinning and tube sheet crevice stress-corrosion problems (ref.2).

3. In the case of U.K. gas cooled reactor steam generators, considerable effort has been directed at understanding and eliminating the possibility of corrosion damage resulting from solute concentration under two phase flow and dryout conditions, and the vulnerability of both Magnox and AGR steam generators to on-load corrosion and stress corrosion has been reviewed very recently (ref.3). The need for stringent feed-water chemical control was recognised and to date they have not proved to be a problem. However, both Magnox and AGR steam generators have been subject to an entirely different type of corrosion damage not dependent on any solute concentration process, namely erosion-corrosion. Similar erosion-corrosion problems have also been encountered in other gas cooled reactors elsewhere, most notably in France and Japan, but the problems are not restricted to gas cooled reactor steam generators, and this type of damage

has occurred in the steam-water circuits of water and sodium cooled reactors. As a result there is growing international interest in erosion-corrosion phenomena (ref. 4-7). The present paper therefore attempts to summarize current experience and understanding of the problem, and describe erosion-corrosion work in progress at CERL.

#### EROSION-CORROSION

4. The term erosion-corrosion is slightly misleading and the phenomenon is perhaps better described as flow assisted corrosion. As such it is clearly distinguishable from pure erosion or cavitation damage.

5. Erosion-corrosion damage normally occurs at locations where there is severe fluid turbulence adjacent to the metal surface, either as a result of inherently high fluid velocities, or the presence of some feature (bend, orifice etc.) generating high levels of turbulence locally. Its occurrence is also usually associated with the use of mild or carbon steel components. The attack occurs under both single and two-phase water conditions, but not in dry steam, which is consistent with the general view that the process is essentially one of surface dissolution. It is frequently, although not invariably, characterized by the occurrence of overlapping horse-shoe shaped pits, giving the surface a scalloped appearance, as shown in Plate 1. However, these pits are normally relatively shallow in comparison to the general metal wastage in the area concerned. The oxide present on the corroding surface is normally very thin, 1 µm or less, and often exhibits a polished appearance. However, heavy oxide deposition is sometimes present on adjacent areas of tube not

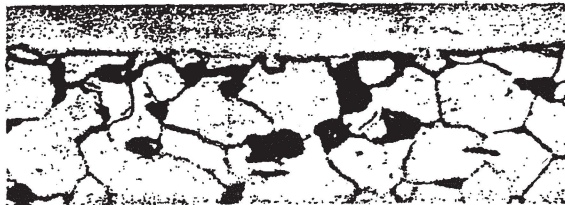


PLATE 1. Erosion-corrosion damage produced under two phase conditions in a mild steel riser pipe from a Magnox steam generator. Flow from left to right.



PLATE 2. Erosion-corrosion damage downstream of the orifice in a CERL mild steel orifice assembly specimen. Flow from left to right.

OXIDE



10 μm

PLATE 3. Metallographic cross section of specimen shown in Plate 2 in region of maximum erosion corrosion loss.

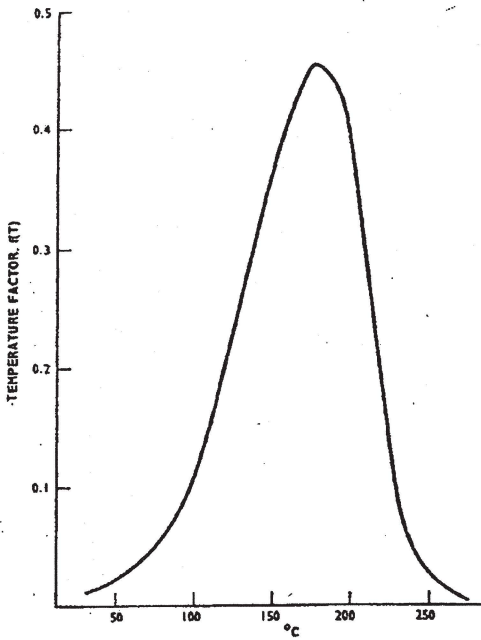


FIGURE 1. Temperature dependence of erosion-corrosion losses under two phase conditions (ref.19)

FLOW PATTERN	REFERENCE VELOCITY	$K_c$	
PRIMARY FLOW STAGNATION POINTS	AT PIPES	1	
	AT BLADES	1	
	AT PLATES	1	
	IN PIPE JUNCTIONS	0.8	
SECONDARY FLOW STAGNATION POINTS	R D 0.5	0.7	
	R D 1.5	0.4	
	R D 3.5	0.3	
	BEHIND PIPE JOINTS	0.3	
STAGNATION POINTS DUE TO VORTER FORMATION	BEHIND SHARP EDGED ORIFICE PIPES	0.3	
	AT AND BEHIND BARRIERS	0.2	
NO STAGNATION POINTS	IN STRAIGHT PIPES	0.04	
	IN UPRIGHT HORIZONTAL TURBINE JOINTS	VELOCITY CALCULATED FROM PRESSURE DROP	0.04
COMPLICATED FLOW THROUGH TURBINE PART	IN TURBINE CLAND SEAL	VELOCITY CALCULATED FROM PRESSURE DROP	0.08
	AT AND ABOVE TURBINE BLADES AND AT DRAINAGE COLLECTING RINGS	AVERAGE CIRCUMFERENTIAL BLADE VELOCITY	0.3

FIGURE 2. Influence of flow path configuration on erosion-corrosion damage under two-phase conditions (ref.13)

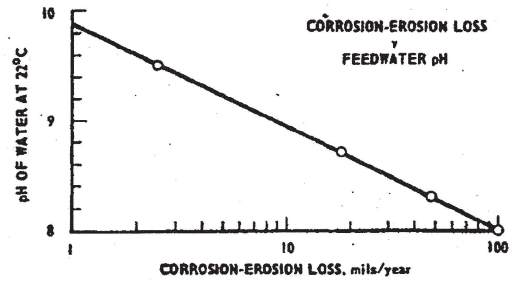


FIGURE 3. Erosion-corrosion loss rate v pH for a rotating disc at 99°C (ref.26)

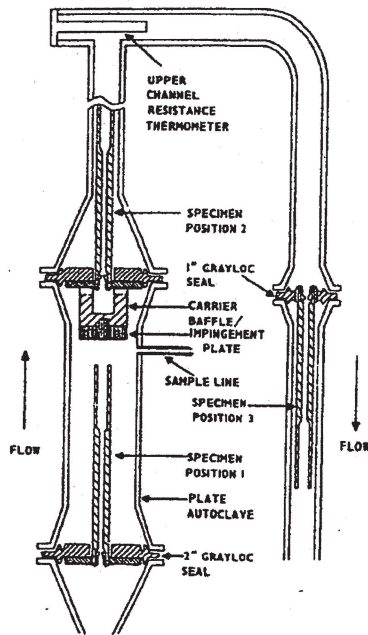


FIGURE 5. Arrangement of orifice assembly specimens in autoclave flow channels.

suffering erosion-corrosion attack, particularly under two phase conditions.

6. Under severe conditions, metal wastage rates of 1 mm/year or even higher can be observed in erosion-corrosion situations, so that component failure can be relatively rapid in the worst cases.

#### Plant Experience

7. Under two phase conditions, erosion-corrosion damage within nuclear steam generators has frequently occurred at tube bends, bifurcations or similar features in the steam-water circuit. Among the earliest reported instances of damage of this type were those at the Tokai Mura plant in late 1968 (ref.8,9). This station employs dual pressure drum recirculation type steam generators, and early failures occurred at 214°C in swan neck bends and tube bifurcations at the outlet end of the mild steel L.P. evaporator tubes. Some failures also occurred at tube bends in the subsequent riser pipes to the L.P. steam drum external to the steam generator itself, and significant tube thinning was reported for the last two return bends of the serpentine evaporator tube banks inside the units. Tube wastage rates as high as 1.3 mm/year were found in some cases. Up to the time of the failures, the boilers had been operated with hydrazine/ammonia dosing to give a boiler water pH in the range 8.5 to 9.2. Some dosing with  $\text{Na}_3\text{PO}_4$  was also employed to combat chloride ion (200-300 ppb) present in the water (ref.9).

8. Similar failures to these have occurred under steaming conditions in the mild steel economiser sections of British Magnox stations, and in the evaporator sections of once-through steam generators such as those at St. Laurent I and II. In the case of St. Laurent II, failures occurred in the 180° return bends of the mild steel serpentine evaporator towards the end of the evaporation zone, at a temperature of about 245°C (ref. 4, 10). As in the case of Tokai Mura, the boiler feedwater was originally dosed with ammonia and hydrazine to about pH 9.0. However, more recently morpholine dosing has been employed because of its lower partition coefficient between water and steam and higher basicity at high temperature, which should maintain a higher solution pH at temperature (ref.11).

9. Erosion-corrosion problems under two phase conditions have also been reported to have occurred in the steam generator units at Marcoule and Chinon 2 (ref.4, 10).

10. Erosion-corrosion damage in nuclear steam generators under single phase (water) conditions has commonly been associated with boiler feedwater tube inlets, and in particular those where orifices have been installed to control the boiler feed flow. Damage of this type has been experienced at St. Laurent II, with an inlet feedwater temperature of about 125°C (ref. 4,10), and at somewhat higher temperature (up to 246°C) in the case of the Phenix steam generators (ref. 5, 10). In the case of Hinkley Point 'B'

Power Station, erosion-corrosion damage at the feedwater inlets downstream of the flow control orifices was compounded by flow bypassing through the gap between the threaded ends of the restrictor tubes and the orifice carriers (ref.12). In some cases this fluid bypassing completely eroded away the restrictor tube end.

11. In addition to problems within the steam generators themselves, erosion-corrosion damage has frequently been encountered in wet steam turbines (ref.13) and associated steam pipework (ref.6), both the feedwater and steam-side of feed heaters (ref.14-17) and boiler feed pumps (ref.7). Clearly therefore the problems are very widespread, and not restricted to any one type of nuclear plant.

#### Current Understanding of Erosion-Corrosion Behaviour

12. In spite of the widespread occurrence of erosion-corrosion problems, as outlined in the preceding section, relatively little experimental or theoretical work on the subject has been reported in the open literature. It is clear, however, that erosion-corrosion behaviour depends on a number of physical and chemical variables. These are principally; materials' composition, local hydrodynamic conditions including the effects of steam quality, temperature and water chemistry. Any model of the process should therefore be capable of explaining the detailed dependence of erosion-corrosion on these parameters. Their general influence on erosion-corrosion behaviour under boiler feedwater conditions is summarised below.

13. Materials' Composition. Erosion-corrosion damage is most frequently observed when carbon or mild steel components are employed. Alloy steels, particularly chrome alloy steels are much less susceptible to erosion-corrosion attack, and austenitic stainless steels essentially immune to damage. Relatively small amounts of chromium in the steel improve its erosion resistance quite markedly, although the degree of improvement appears to depend on the severity of the conditions. Thus in tests at 120°C, involving impingement of a water jet on the sample surface at 58 ms<sup>-1</sup>, 2% Cr steel was found to be at least an order of magnitude more resistant to damage than carbon steel, with higher chrome steels even more resistant (ref.18). However, practical experience with wet steam turbines and their associated pipework suggests 2½% Cr steel to be about four times more resistant to attack than mild steel, whilst 12% Cr steel has proved to be virtually unaffected (ref.13).

14. It is likely that other minor alloying or trace elements such as copper, nickel, manganese and silicon would influence resistance to erosion-corrosion as such elements are known to affect corrosion resistance of carbon and low alloy steels to a wide range of aqueous environments. However, there appears to be no systematic studies reported in the open literature.

15. Temperature. Erosion-corrosion damage is most prevalent in the temperature range 50° to 250°C. Fig. 1 shows the effect of temperature on relative erosion rates based on data derived from damage occurring under two phase conditions in wet steam turbines (ref.19). This indicates maximum damage to occur at around 180°C. However, more recently it has been proposed that under single phase conditions, the maximum is close to 140°C (ref.20). Limited studies on the effects of temperature under single phase conditions have also been reported by Decker, Wagner and Marsh (ref.21) which would appear to support this, but there remains some uncertainty in the precise variation of erosion-corrosion rates with temperature. For example, rapid two phase erosion damage has frequently been observed at temperatures well in excess of 200°C (e.g. St. Laurent II), whereas the curve in Fig. 1 would suggest the problem to be disappearing rapidly at these temperatures.

16. Hydrodynamics. Erosion-corrosion damage has in general been observed at points of hydrodynamic disturbance in the fluid flow. Under single phase conditions damage has frequently occurred at tube entries in preheaters, or downstream of orifices at boiler tube entries, whereas under two phase conditions the damage has often been associated with bends. Keller (ref.19) has attempted to rationalize the effects of various flow path configurations on erosion-corrosion damage under two phase conditions by use of an empirical damage factor ( $K_c$ ) together with a reference flow velocity. These are given in Fig. 2. However, it is doubtful that these parameters can be equally well applied to damage under single phase conditions as a result of the differing hydrodynamic flow patterns which would occur. More recently at CERL and elsewhere (ref.7) attempts have been made to relate erosion-corrosion rates in single phase water to local mass transfer rates, and these will be discussed subsequently.

17. In view of the critical dependence of erosion-corrosion damage on fluid flow and turbulence, it is surprising that no detailed studies have been reported of the effect of flow velocity and turbulence on erosion-corrosion rates. Some studies have been made at high temperature (>280°C) (ref.22-24), but these are outside the range normally associated with erosion-corrosion attack.

18. Water Chemistry. Several aspects of water chemistry are thought to influence erosion-corrosion behaviour. The effect of pH and oxygen content of the water have been examined, but other components such as hydrazine and dissolved iron are also expected to exert a significant influence on the process (ref.25).

19. Most instances of erosion-corrosion damage have occurred with a deoxygenated volatile alkali dosed water chemistry.

20. In studies of erosion-corrosion damage in feed heaters (ref.14,15), it was found that attack occurred predominantly when the feedwater

pH was less than 9.0, but attack was not normally observed with pH >9.2. Similarly, the occurrence of erosion-corrosion damage in wet steam turbines has been reported to occur only when the condensate pH is below about pH 9.4 (ref.13,19).

21. The effect of pH on erosion-corrosion rates has been studied experimentally by Apblett (ref.26) using a rotating carbon steel disc over the pH range 8.0 to 9.5 at 99°C in deaerated water. The results are shown in Fig. 2, and indicate a tenfold reduction in wastage rate on increasing the pH from 8 to 9. Similar reductions in rate have also been reported for jet impingement studies at 120°C (ref.27).

22. The effect of oxygen on erosion-corrosion behaviour as such has not been studied in great detail. However, iron release rates from carbon steel in neutral water at 1.85 ms<sup>-1</sup> over the temperature range 38° to 204°C have been shown to decrease by up to two orders of magnitude with increasing oxygen content over the range <1 to 200 ppb (refs.23, 28-31). It is to be expected that erosion-corrosion will at least qualitatively follow this type of behaviour.

23. Additions of up to 300 ppb oxygen (or more commonly hydrogen peroxide) to neutral feedwater forms the basis of the neutral oxygen low conductivity (NOLC) water chemistry regime used by a number of power utilities for fossil fired once thro' boilers (ref.32), and these are evidently largely free from erosion-corrosion damage. More recently, it has been reported that combined NH<sub>3</sub>/H<sub>2</sub>O<sub>2</sub> dosing of feedwater is also effective in this respect (ref.33).

#### Models of Erosion-Corrosion Behaviour

24. Keller (ref.19) has proposed an empirical equation for predicting erosion-corrosion losses from carbon steel, based on observations in wet steam turbines. This has the form

$$s = f(T).f(x).c.K_c - K_s \quad (1)$$

where s is the maximum local depth of material loss in mm/10<sup>4</sup> hours.

f(T) is a dimensionless variable denoting the influence of temperature on erosion-corrosion damage. A plot of f(T) is shown in Fig. 1.

f(x) is a dimensionless variable denoting the influence of steam wetness on erosion-corrosion loss. For sub-cooled water it has been suggested that this has a value of unity, but for two phase mixtures it has the form  $f(x) = (1 - x)^{K_x}$ , where x is the steam fraction and  $0 \ll K_x < 1$ . A value of  $K_x = 0.5$  is evidently considered the most appropriate one.

$K_c$  is a variable factor accounting for the effect of local geometry on the fluid flow. Values of  $K_c$  in mm.s/m 10,000 hours are

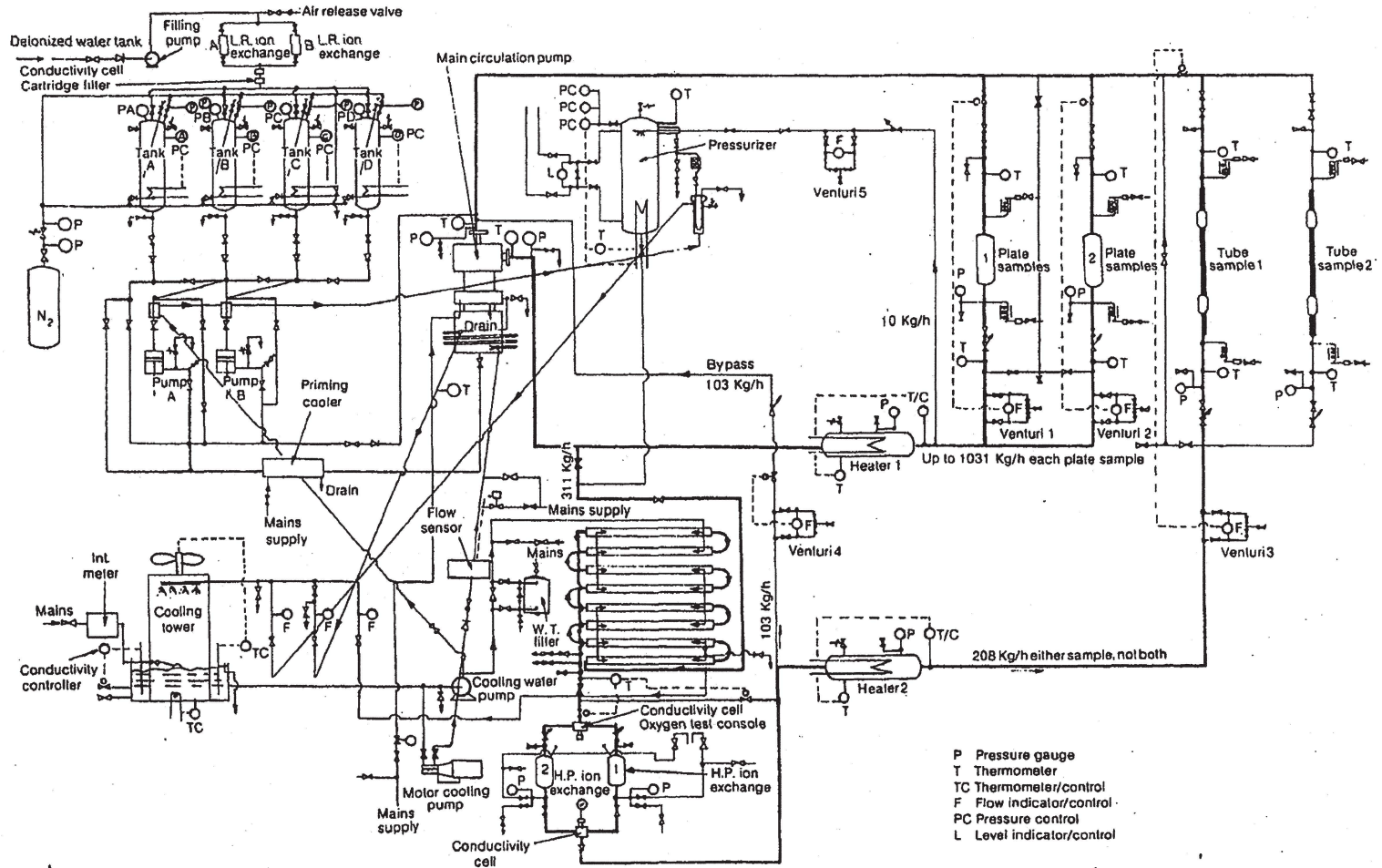


FIGURE 4. Isothermal Rig flow diagram

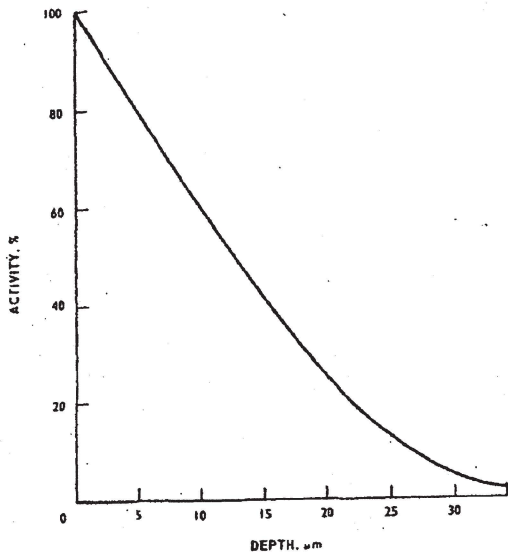


FIGURE 6. Activity/depth curve for  $^{56}\text{Co}$  produced in an iron matrix by a 10.8 MeV proton beam inclined at  $10^\circ$  to the surface

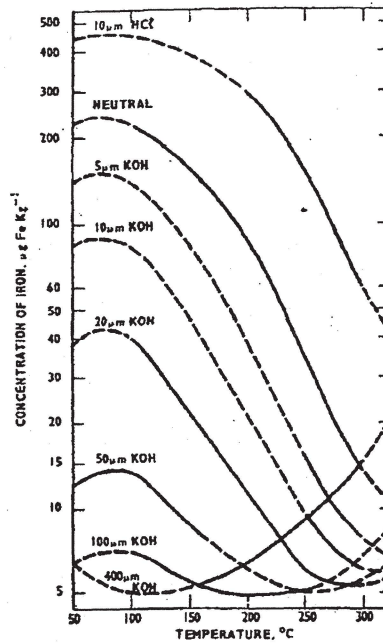


FIGURE 8. Variation of magnetite solubility with temperature and pH at 1 bar hydrogen partial pressure. (Ref. 42)

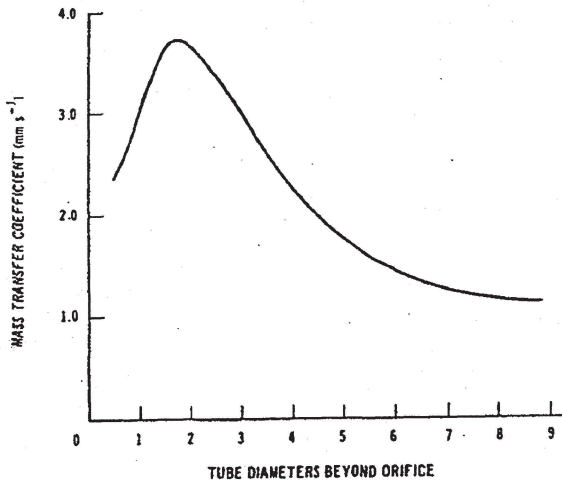


FIGURE 7. Variation of mass transfer coefficient in a tube downstream of an orifice

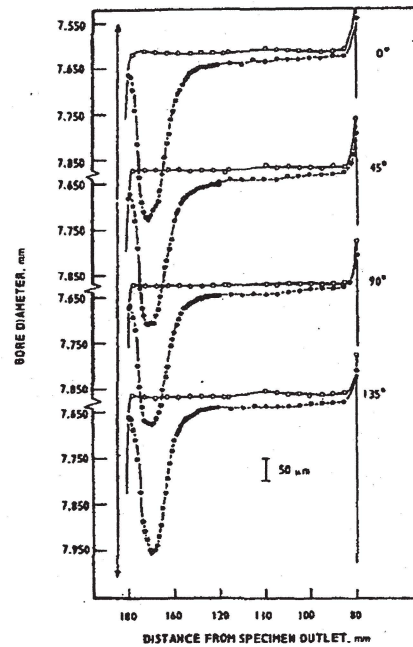


FIGURE 9. Erosion-corrosion loss profile in tube downstream of an orifice (Diametral circumferential locations shown. Orifice located 185 mm from specimen outlet)

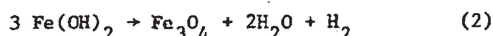
given in Fig. 2.

c is the fluid velocity in  $\text{ms}^{-1}$ .

$K_s$  is a constant which the first term must exceed before erosion-corrosion is observed. A value of  $1 \text{ mm}/10^4$  hours has been given by Keller (ref.19).

Equation (1) does not include any influence from changes in water chemistry, although as indicated earlier, these have a very marked effect on the rate and occurrence of erosion-corrosion damage. It is also very doubtful that it can be applied in its present form to single phase erosion-corrosion damage, since many instances of damage have occurred under single phase conditions which would not have been predicted by equation (1).

25. Discussions of some mechanistic aspects of erosion-corrosion attack has been given by Homig (ref.34) and Bohnsack (ref.35), who concluded that the process is due to dissolution of the metal surface to give  $\text{Fe}^{2+}$  ions in solution, which are continually removed by the turbulent fluid flow. However, both these authors restrict themselves largely to discussion of the dissolution at  $25^\circ\text{C}$ , which is well below the temperatures at which erosion-corrosion attack is normally encountered. At  $25^\circ\text{C}$ ,  $\text{Fe}(\text{OH})_2$  is normally considered to be the corrosion product involved in the dissolution process in deoxygenated water, but at temperatures higher than about  $100^\circ\text{C}$ , this is converted to  $\text{Fe}_3\text{O}_4$  via the Schikorr reaction:



The rate of this reaction increases with temperature, and magnetite is typically the phase observed on surfaces undergoing erosion-corrosion attack at temperatures above about  $120^\circ\text{C}$ . As a result, erosion-corrosion attack at these higher temperatures has been attributed to rapid dissolution of the unstable  $\text{Fe}(\text{OH})_2$  intermediate (ref.36).

26. Very recently attempts to produce a model of erosion-corrosion based on calculated mass transfer rates and the solubility of magnetite have been made by Gülich et al. (ref.7). Work to produce a more satisfactory model is also in progress at CERL, and this is outlined in subsequent sections. However, at present there is no completely satisfactory model of erosion-corrosion behaviour which is capable of rationalizing the effect of all the diverse factors influencing the process.

#### CERL EROSION-CORROSION STUDIES

27. The work currently in progress at CERL on erosion-corrosion is directed at establishing a consistent set of experimental data from which it is possible to make accurate predictions of plant behaviour, and to develop a satisfactory theoretical model of the process capable of rationalizing the experimental work. At present, both experimental and theoretical studies are concerned entirely with erosion-corrosion in single phase water, although it is to be hoped that the results of the work can be applied with certain limitations to erosion-corrosion

behaviour under two-phase conditions.

#### Experimental Facility

28. Experimental studies of erosion-corrosion are being carried out using a high velocity isothermal water circulation loop, referred to as the isothermal rig for short (ref.37). This facility consists basically of a main circulation loop, a secondary water clean up loop and a pressurizer loop, together with ancillary make-up/dosing and chemical sampling systems. A flow diagram for the rig is shown in Fig. 4.

29. Four specimen flow channels are incorporated in the rig, two specimen autoclaves in the main loop, and two tube specimens within the secondary polishing loop.

30. The rig is principally constructed of Type 316 stainless steel, with the exception of the pressurizer vessel ( $2\frac{1}{2}$  Cr 1 Mo ferritic steel), the heater elements (Inconel) and some parts of the main circulating pump (Incoloy 825, stellite and ferobestos). The rig is designed to operate over the following range of physical conditions:

Temperature,	up to $350^\circ\text{C}$
Pressure,	up to $21.78 \text{ MNm}^{-2}$ ( $3160 \text{ lbf in}^{-2}$ )
Autoclave flowrates,	up to $1031 \text{ kg h}^{-1}$ per autoclave
Tube specimen flowrate,	up to $208 \text{ kg h}^{-1}$ total
Bypass flowrate,	up to $103 \text{ kg h}^{-1}$
Pressurizer flowrate,	up to $20 \text{ kg h}^{-1}$

Once the rig water has been pressurized and water circulation achieved using the main pump, control of the physical operating parameters of the rig is largely automatic, with the variables of interest (flow rate, temperature, pressure, water level etc.) being recorded by a dedicated CAMAC data logger.

31. The rig incorporates four methods for controlling the water chemistry, namely ion exchange, chemical dosing, blowdown and deaeration. Data on the chemical composition of the water within the rig is derived mainly from continuous chemical monitoring of sample streams which can be drawn from a large number of different sampling points around the rig. The exception to this is the direct measurement of conductivity before and after the ion-exchange columns. To date, all the experimental work carried out on the rig has been with an ammonia dosed deoxygenated water chemistry regime, and for these conditions it has been found convenient to work with the cation exchange resins of the mixed bed ion-exchange columns converted to their ammonium ion form.

32. In its present form, the rig is capable of operating within the following limits of physical and chemical control parameters.

Temperature at test specimens	$\pm 1^{\circ}\text{C}$
Flow to test specimens	$\pm 1\%$
pH of circulation water*	$\pm 0.1$ pH unit
Conductivity of water after cation exchange+	$< 0.6 \mu\text{S cm}^{-1}$
Dissolved iron in circulating water at $148^{\circ}\text{C}$	$< 10 \mu\text{g kg}^{-1}$
Dissolved active silica in circulating water at $148^{\circ}\text{C}$	$< 10 \mu\text{g kg}^{-1}$
Dissolved oxygen in circulating water at $148^{\circ}\text{C}$	$< 6 \mu\text{g kg}^{-1}$

\* Dependent on pH of circulating water, values given for pH 9.0. At higher pH, the precision of pH control improves, and dissolved Fe levels fall.

+ Upper limit of conductivity, due to very slow sampling rate.

#### Test Specimens

33. A variety of erosion-corrosion test specimens can be incorporated into the isothermal loop, using both the autoclave and tube specimen flow channels.

34. The tube specimen channels are provided with couplings for the attachment of tubing between two points 2 m apart. Initially straight 3 mm bore mild steel test specimens and stainless steel dummy specimens have been incorporated, but it is possible to incorporate bent tubes, bore expansions and constrictions and a variety of other options in this area of the rig.

35. Four plate type specimens,  $195 \times 12 \times 1$  mm can be incorporated into each of the autoclave flow channels using stainless steel specimen holders. These hold the specimens with a 1 mm gap between them, and allow rig water to flow along their length. However, it is possible to incorporate other types of test specimens in the autoclave flow channels, and most of the work to date has involved the use of orifice assembly specimens. Up to three such assemblies can be accommodated in each autoclave flow channel, as shown in Fig. 5. To minimise interaction between specimens in series with one another, a baffle plate can be inserted, as shown in Fig. 5, and this also serves as an impingement specimen. It is possible to incorporate up to three orifice assemblies in parallel on the inlet Grayloc seal of the autoclave, and in this way interactions between adjacent tubes could be studied, in addition to increasing the total number of specimens. This does, however, reduce the flow through any one specimen to one third of that through the specimen on the autoclave outlet Grayloc seal.

36. The advantage of using this type of orifice assembly is that experiments can be performed on specimens which accurately simulate plant components, and which are well characterised

hydrodynamically. They can therefore be used for precise correlation of erosion-corrosion and mass transfer behaviour (see subsequent discussion). The particular specimens used permit behaviour to be studied at five different potential erosion-corrosion sites; the tube inlet, the jet reattachment zone downstream of the orifice, downstream of a tube expansion, and in two different diameter straight tube sections (i.e. two different flow velocities). The specimens also have the advantage that being essentially straight tube test pieces, it is possible to use high accuracy bore diametral measurements to characterize the erosion loss profile throughout the specimen.

#### Erosion-Corrosion Monitoring Methods

37. Simple weight change measurements are possible on all the test specimens described, except the tube specimen channels themselves. However, most of the effort to date has been concentrated on monitoring damage produced in the orifice assembly specimens, and this has been done principally by the use of high accuracy bore diametral measurements, and thin layer surface activation methods.

38. Bore Metrology. Measurements of bore diameter have been made on test specimens using a "Diatest" internal bore measuring instrument. This instrument permits diametral measurements to be made with a precision of  $\pm 1 \mu\text{m}$ , and on a uniform tube surface, the reproducibility was better than  $\pm 2 \mu\text{m}$ . The tubes used in the present work are typically either drawn, or machined from bar material and have a honed surface finish. In both cases, the quality of the tubes used is sufficiently good to permit measurements to be made with the reproducibility quoted above.

39. On non-uniform tubes, or heavily eroded surfaces where the diameter changes rapidly, the reproducibility of measurement is reduced, principally due to the relatively poor longitudinal precision ( $\pm 0.5$  mm) with which measurements are made at present. Measures are currently in hand to improve this by using an automated measuring procedure. Nevertheless, in all cases to date it has been possible to produce highly accurate bore loss profiles from the test specimens.

40. Surface Activated-Specimens. Erosion-corrosion losses of a number of specimens have been monitored in situ by the use of thin layer activation of the specimen. To date this has only been employed with orifice assemblies, but can in principal be used for any type of specimen.

41. The technique consists of activating to a known depth an area of the specimen surface by high energy charged particle bombardment (ref.38). Metal loss from the specimen can then be determined by monitoring the loss in activity from the specimen surface as erosion-corrosion proceeds. In the present work, small areas of the internal tube surface ( $5$  to  $10$  mm  $\times$   $1.75$  mm) have been activated by bombardment with  $10.8$  MeV protons at angles of  $10^{\circ}$  or  $20^{\circ}$  to the tube surface.

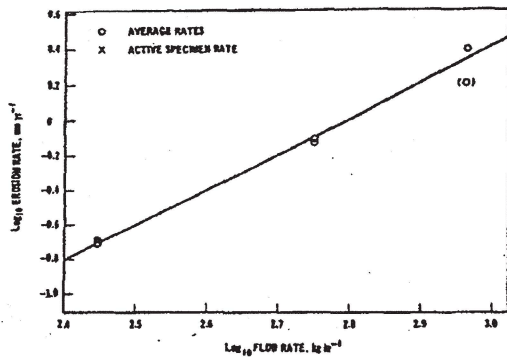


FIGURE 10. Velocity dependence of maximum erosion-corrosion rate observed downstream of an orifice at 157°C, and pH 9.05

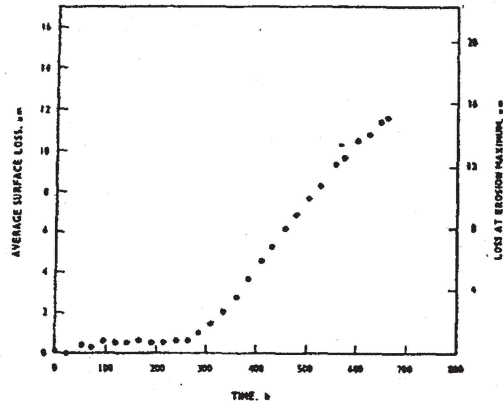


FIGURE 12. Time dependence of erosion-corrosion loss for a surface activated specimen.

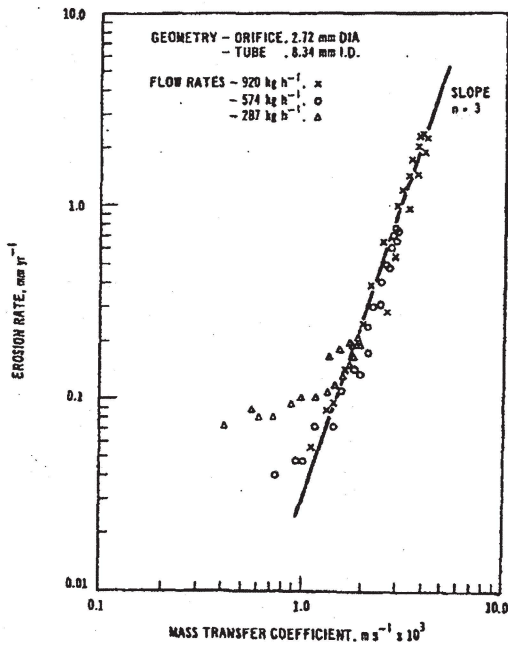


FIGURE 11. Correlation of erosion corrosion rate downstream of orifice with corresponding mass transfer coefficient throughout the erosion-corrosion zone

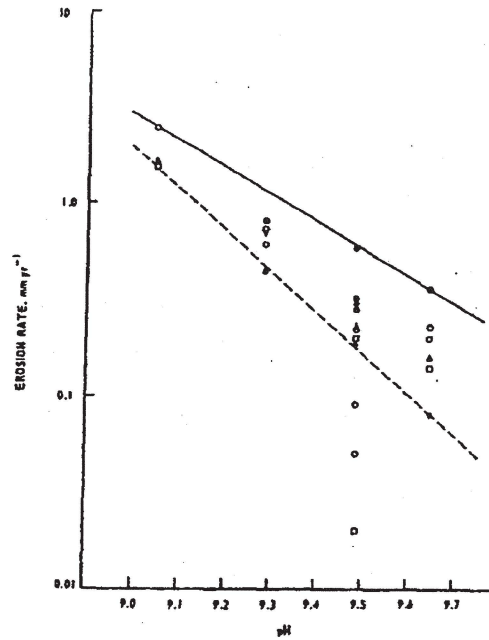


FIGURE 13. pH dependence of erosion-corrosion rates at 157°C. Solid symbols, maximum rates from surface activated specimens, open symbols average rates

The bombardment of  $^{56}\text{Fe}$  with high energy protons produces  $^{56}\text{Co}$  which has a half-life of 77.3 days, and the principal  $\gamma$ -ray emitted on decay has an energy of 845 keV. The maximum depths of activation for bombardment with protons at  $10^\circ$  and  $20^\circ$  are around 35 and 70  $\mu\text{m}$  respectively. Deeper activation is possible by bombarding normally to the tube surface, or by increasing the incident proton energy. The total  $^{56}\text{Co}$  activity versus depth curve for bombardment at  $10^\circ$  to the tube surface is shown in Fig. 6.

42. Loss of material from the specimen surface has been determined in-situ by monitoring the  $\gamma$ -ray emissions from the sample using a scintillation detector placed in close proximity to the autoclave containing the active specimen. These have permitted measurements of erosion loss to be made as a function of time with an accuracy of  $\pm 0.1 \mu\text{m}$  in the case of an activation depth of 35  $\mu\text{m}$ .

43. Full details of the experimental technique will be reported elsewhere (ref.39).

#### Theoretical Work

44. If erosion-corrosion is controlled solely by the rate of mass transfer of Fe from the eroding surface, then the erosion-corrosion rate may be expected to vary according to

$$\frac{dm}{dt} = K(C_s - C_b) \quad (3)$$

Where K = mass transfer coefficient

$C_s$  = concentration of iron in solution at the oxide-solution interface

$C_b$  = concentration of iron in the bulk solution

$\frac{dm}{dt}$  = rate of metal loss.

45. The value of the mass transfer coefficient K varies with the local hydrodynamic conditions. Its dependence on these is usually expressed in dimensionless form using the corresponding Sherwood number Sh, where  $Sh = KD/D$ , D = duct diameter and  $D$  = diffusion coefficient for iron in solution. This is normally expressed in terms of the Reynolds (Re) and Schmidt (Sc) numbers in empirical correlations of the form

$$Sh = \alpha Re^\beta Sc^\gamma \quad (4)$$

where  $\alpha$ ,  $\beta$  and  $\gamma$  are constants determined by experiment;  $\gamma$  typically has a value around 1/3, whilst the value of  $\beta$  is usually in the range 2/3 to 7/8. Correlations of this type are already available for a number of hydrodynamic situations of concern in erosion-corrosion, and two of particular interest in the present work are those for turbulent flow in straight pipes (ref.40), and downstream of an orifice (ref.41). These have the form:

$$\text{Straight pipes: } Sh = 0.0165 Re^{0.86} Sc^{0.33} \quad (5)$$

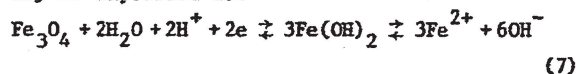
$$\text{Downstream of an orifice: } Sh_{\max} = 0.27 Re_N^{0.67} Sc^{0.33} \quad (6)$$

where Sh<sub>max</sub> in equation (6) refers to the maximum Sherwood number observed downstream of the orifice, and  $Re_N$  the orifice Reynolds number. The overall variation of mass transfer coefficient K in the tube downstream of the orifice is illustrated in Fig. 7.

46. The value of  $C_b$  in equation (3) may clearly be determined experimentally for any given erosion-corrosion situation, and for most situations of practical interest will be very low, probably less than  $10 \mu\text{g kg}^{-1}$ . However, the concentration of iron in solution at the oxide-solution interface cannot be so easily evaluated. In the first instance, it might be assumed that this term may be equated with the equilibrium solubility of the surface oxide, which at temperatures above about  $100^\circ\text{C}$  is usually taken to be magnetite. If however some metastable intermediate oxide such as  $\text{Fe}(\text{OH})_2$  is invoked, then a different solubility would be appropriate.

47. The solubility of magnetite is known to be dependent on temperature, pH and hydrogen partial pressure (ref. 42). Fig. 8 shows the variation in magnetite solubility with pH and temperature at 1 bar partial pressure of hydrogen ( $1585 \mu\text{g kg}^{-1}$ ) derived from the data of Sweeton and Baes. However, these solubilities are much higher than would be anticipated in operating plant, where the partial pressure of hydrogen would be much lower ( $\sim 5 \mu\text{g kg}^{-1}$ ). Under these circumstances the equilibrium solubility of magnetite, when taken with the expected mass transfer coefficients is far too low to explain the observed erosion-corrosion rates (ref.43). This analysis would indicate that the solubility of the surface oxide is much higher than that expected for magnetite in equilibrium with the bulk partial pressure of hydrogen. It is possible, however, that the solubility may be sufficiently enhanced locally by the high equivalent partial pressure of hydrogen which results from the high local corrosion rate. Once established, the high local solubility in turn assists in maintaining the high erosion rate. Electrochemically this is equivalent to the dissolution process occurring at relatively negative potentials, which is in agreement with the general observation that actively eroding areas are normally covered with magnetite, whereas nearby non-eroding surfaces are frequently covered with haematite. This possibility may be analysed theoretically in the following manner:

48. At equilibrium, the dissolution of magnetite to form  $\text{Fe}^{2+}$  ions in solution (the dominant species under the conditions of interest) may be expressed as:



for which the appropriate Nernst-equation is

$$E = E^\ominus - \frac{RT}{2F} \ln \frac{[\text{Fe}(\text{OH})_2]^3}{[\text{H}^+]^2} \quad (8)$$

which gives

$$[\text{Fe}^{2+}] = \frac{[\text{H}^+]^{8/3}}{K_2} \exp\left(\frac{-2F(E - E^0)}{3RT}\right) \quad (9)$$

$$\text{where } K_2 = \frac{[\text{Fe(OH)}_2][\text{H}^+]^2}{[\text{Fe}^{2+}]}$$

The cathodic current  $i_c$  of the corrosion reaction resulting from hydrogen discharge at the surface of the magnetite film may be expected to vary exponentially with the surface potential  $E$  of the film, as follows:

$$i_c = -FB \exp\left(-\frac{\beta FE}{RT}\right) \quad (10)$$

If the anodic current  $i_a$  at this potential is limited by the rate of removal of  $\text{Fe}^{2+}$  ions from the surface, and since  $i_a + i_c = 0$ ,

$$2FK \left\{ [\text{Fe}^{2+}] - C_b \right\} = FB \exp\left(-\frac{\beta FE}{RT}\right) \quad (11)$$

If  $C_b \ll [\text{Fe}^{2+}]$  and  $\beta = 1$  then substituting from equation (9) and eliminating  $E$  gives

$$[\text{Fe}^{2+}] = \frac{4K^2 [\text{H}^+]^8}{K_2^3 B^2} \exp\left(\frac{2FE^0}{RT}\right) \quad (12)$$

In this case the  $\text{Fe}^{2+}$  solubility of magnetite at the surface is dependent on the square of the mass transfer coefficient  $K$ , giving an overall dependence of the erosion rate on the cube of the mass transfer coefficient, through equation (3).

49. This treatment may be extended to include all soluble iron species under the conditions of interest, and the effects of a non negligible bulk concentration of iron. The expressions become more complex in this case, but still indicate a dependence of erosion-corrosion rate on the cube of the mass transfer coefficient (plus smaller terms in  $K^2$  and  $K$ ). Further analysis of the mechanistic aspects of erosion-corrosion is still under consideration, but this rather unexpected dependence of the rate on the cube of the mass transfer coefficient is born out by experiment.

## Results

50. Plate 2 shows the erosion-corrosion zone downstream of the orifice generated in a mild steel orifice assembly test specimen. Although the surface loss at the erosion maximum is relatively large ( $\sim 150 \mu\text{m}$ ), scalloping of the surface, of the type shown in Plate 1 has not yet developed. However, the oxide film present in the eroded area is extremely thin, as shown in Plate 3.

51. In the case of specimens undergoing very rapid erosion-corrosion wastage, the films are sufficiently thin to exhibit interference colours. With lower erosion-corrosion rates, however, the eroding surface is black, as for non-eroding areas of the tube surface.

52. Micropitting of the tube surface to a depth of about  $5 \mu\text{m}$  is evident in the erosion zone shown in Plate 3, and this is associated with accelerated attack of the pearlite grains of the steel. Effects of this type have also been observed in plant specimens.

53. Most of the work to date has involved the use of mild steel orifice assembly specimens, and Fig. 9 shows a typical erosion-corrosion loss profile downstream of the orifice, obtained using the bore measuring technique outlined previously. The general similarity to the mass transfer profile shown in Fig. 7 is immediately apparent. However, it is clear that the straight tube losses are quite small, whereas Fig. 7 shows the mass transfer coefficient decays asymptotically to that appropriate to the straight tube, which is about 1/3 to 1/4 of that at the mass transfer maximum. It is important to note however, that the maxima in both curves occurs approximately 2 tube diameters beyond the orifice.

54. Experiments exposing several specimens at different flow rates under the same conditions may be used to establish the flow and hence mass transfer dependence of the erosion rate, and Fig 10 shows the velocity dependence obtained at  $148^\circ\text{C}$  using pairs of specimens at three different flow rates. The slope the plot indicates a  $V^2$  dependence of erosion rate on flow, which according to equation (6) would indicate a dependence on mass transfer coefficient cubed. Further confirmation of this  $K^3$  dependence is shown in Fig. 11, where the erosion loss profiles of individual specimens have been compared point by point with the corresponding mass transfer profile of the type shown in Fig. 7. From this it is seen that not only do the maximum losses downstream of the orifice conform with the  $K^3$  dependence, but the erosion-corrosion rates over nearly the whole profile of the specimens correlate with  $K^3$ .

55. Whilst this alone does not substantiate the theoretical treatment outlined in the previous section, it does provide strong support for the type of mechanism invoked, and indicates that further development of the theory along these lines should prove very fruitful.

56. Fig. 12 shows the erosion-corrosion loss of an orifice assembly specimen downstream of the orifice as a function of time, determined from the activity loss of a surface activated spot in the erosion-corrosion zone. It is evident that under the particular conditions used, there is a substantial initiation time before any erosion-corrosion loss is observed. Once initiated, the erosion-corrosion rate rose rapidly to a high value, and then remained constant for most of the remainder of the test (the reduction in rate towards the end of the

test shown in Fig. 12 is thought to be due to changes in experimental conditions). This type of behaviour has been observed on a number of occasions, although the initiation time can vary widely with the experimental conditions, generally being much shorter under more aggressive erosion-corrosion conditions. The cause of such initiation periods is not certain at present. In some cases this most likely represents the time taken to remove a thin oxide film produced during start-up of the rig, when specimens are exposed to low flow for a few hours. In other cases it is thought that thin air formed oxides produced during welding of the test specimens were responsible. However, in some cases, an initial loss of a few microns has been observed, after which no loss has occurred for up to 200 hours, before true erosion-corrosion attack has been initiated with a continuing linear loss as a function of time. This would suggest that initiation is more complex than simply removing a pre-existing oxide film, and may indicate changes occur in initially formed films under erosion-corrosion conditions.

57. The pH dependence of erosion-corrosion rates has also been investigated using orifice assemblies and Fig. 13 shows the results obtained at 148°C. The upper limit of the data is essentially derived from the maximum linear rates observed using surface activated specimens. The rates derived from other specimens are average rates, which are in general lower as a result of a significant but unknown initiation time. The erosion-corrosion rates decrease by a factor of about 7 over the pH range 9.05 to 9.65, which is equivalent to a variation with  $[H^+]^{1.4}$ . This is a somewhat higher dependence than that seen by Apblett (ref.26) at 99°C, where the erosion-corrosion rate varies as  $[H^+]^{1.0}$ .

#### SUMMARY

58. Corrosion resulting from salt concentration caused by evaporation continues to be a major cause of steam generator damage, particularly in PWRs and has been the subject of intense international research. Erosion-corrosion damage has occurred in a wide variety of nuclear steam generators, but unlike corrosion resulting from solute concentration, relatively little work on the problem has been reported in the open literature. The available experience, previous research and current understanding of the phenomenon have been reviewed, and CERL research on the subject summarized.

59. The CERL isothermal loop has been used to study erosion-corrosion behaviour under single phase conditions comparable with those which occur in plant. By using test specimens which are well characterised hydrodynamically, it has been possible to accurately correlate erosion-corrosion rates with the corresponding mass-transfer rate. Under the particular conditions used (148°C, pH 9.05), it has been found that the rate varies as the cube of the mass-transfer coefficient. This unexpected result is explicable, however, in terms of an electro-chemically based model of magnetite dissolution.

60. Since mass-transfer coefficients can be calculated for a wide variety of hydrodynamic situations, at least under single phase conditions, it should be possible to use correlations of this type to predict plant behaviour over a wide range of conditions.

61. Increasing pH has been shown to markedly reduce erosion-corrosion rates over the range 9.05 to 9.65, in agreement with other studies of the effect at lower temperatures. In many plant situations, therefore, this option should prove effective in controlling erosion-corrosion damage. It is likely to be especially useful when other options such as materials change or oxygen addition are not feasible.

62. Details of the mechanism of erosion-corrosion damage have still to be established, but the use of surface activation in the present work has proved to be extremely valuable for monitoring losses in-situ. Using this technique it has been possible to establish the linearity of erosion-corrosion loss as a function of time, after some initiation period, and it will undoubtedly be useful in studying erosion-corrosion behaviour under transient conditions. In conjunction with electrochemical techniques, therefore, it should prove very valuable in elucidating aspects of the corrosion mechanism.

#### ACKNOWLEDGEMENTS

63. We wish to thank J.H. Ashford, C.H. de Whalley, D. Libaert and R. Sale for their assistance with the experimental work described, and M.W.E. Coney for helpful discussions on aspects of mass-transfer behaviour in turbulent flow.

64. This paper is published with the permission of the Central Electricity Generating Board.

#### REFERENCES

1. GARNSEY R. Boiler corrosion and the requirement for feed- and boiler-water chemical control in nuclear steam generators. BNES Conference on Water Chemistry of Nuclear Reactor Systems, BNES, London, 1978, pp 1-10.
2. GARNSEY R. Nucl. Energy 18, 117, 1979.
3. GARNSEY R. Reducing the risk of water-steam corrosion damage in U.K. Gas cooled reactor steam generators. Paper presented to ADERP meeting on Water Chemistry and Corrosion in the Steam-Water Loops of Nuclear Power Stations, Seillac, March 1980.
4. CHANUDET L. Generateurs de vapeur chauffés au gaz carbonique dans les centrales nucléaires Françaises. Paper presented to ADERP meeting on Water Chemistry and Corrosion in the Steam-Water Loops of Nuclear Power Stations, Seillac, March 1980.
5. ROBIN M.G. SALON G. and ZUBER T. Les generateurs de vapeur pour reacteurs a neutrons rapides. Paper presented to ADERP meeting on Water Chemistry and Corrosion in the Steam-Water Loops of Nuclear Power Stations, Seillac, March 1980.
6. GERDAN J.F. GREGOIRE J. and LACAILLE L. Observations des phenomenes d'erosion-corrosion en vapeur humide-parametres influents et remedes

- possibles. Paper presented to ADERP meeting on Water Chemistry and Corrosion in the Steam-Water Loops of Nuclear Power Stations, Seillac, March 1980.
7. GULICH J.F. FLORJANCIC D. and MULLER E. L'erosion-corrosion dans les pompes d'alimentation et d'extraction. Recherches et choix des materiaux. Paper presented to ADERP meeting on Water Chemistry and Corrosion in the Steam-Water Loops of Nuclear Power Stations, Seillac, March 1980.
  8. Japan Atomic Power Company Limited, Third technical collaboration report on S.R.U. tube erosion and corrosion at the Tokai Nuclear Power Station, J.A.P.C. Report, November 1969.
  9. Japan Atomic Power Company Limited, Fourth Technical Collaboration Meeting on S.R.U. repair work at the Tokai Nuclear Power Station, J.A.P.C. Report, September 1970.
  10. GARAUD J. Revue Generale Nuclaire, No. 1, p. 29, 1978.
  11. BERGE Ph. and SAINT PAUL P., Electricite de France Report HC PV D 389 MAT/T.42.
  12. PASK D.A. and HALL R.W. Nuclear Energy, 18, 237, 1979.
  13. ENGELKE W. in 'Two Phase Steam Flow in Turbines and Separators', ed M.J. MOORE and C.H. SIEVERDING, McGraw-Hill, p. 291-315, 1976.
  14. PERGOLA A.C. and PHILLIPS A. Heat Engineering, p. 72, September-October 1965.
  15. PHILLIPS H. Foster Wheeler Corporation (New Jersey), Report No. TR-36, 1966.
  16. KELP F. MITT V.G.B. 49, 424, 1969.
  17. DOR F. Revue Generale Thermique, 166, 705, 1975.
  18. WAGNER H.A. DECKER J.M. and MARSH J.C. Trans. ASME 69, 389, 1947.
  19. KELLER H. V.G.B., Kraftwerkstechnik, 54, 292, 1974.
  20. KELLER H. J. Internationales D'Etudes Des Centrales Electrique, Paper 42, 1978.
  21. DECKER J.M. WAGNER H.A. and MARSH J.C. Trans. ASME 72, 19, 1950.
  22. WARZEE M. DARLODOT P.de and WATY J. EURATOM Report No. EUR 2688.F., 1966.
  23. NESMEYANOVA K.A. Atomnaya Energiya, 29, 781, 1970.
  24. BERGE P. ADERP Conference, Ermenonville, 1972.
  25. BIGNOLD G.J. JOHN W. and WOOLSEY I.S. Paper to this Conference.
  26. APBLETT W.R. Proc. Am. Power Conf. 29, 751, 1967.
  27. DECKER J.M. and MARSH J.C. Trans. ASME, 72, 19, 1954.
  28. BRUSH E.G. and PEARL W.L. Proc. Am. Power Conf. 31, 699, (1969).
  29. BRUSH E.G. and PEARL W.L. Proc. Am. Power Conf. 32, 751, (1970).
  30. BRUSH E.G. and PEARL W.L. Corrosion 28, 129, 1972.
  31. VREELAND D.C. GAUL G.G. and PEARL W.L. Corrosion 17, 269t, 1961.
  32. FREIER R.K. V.G.B. Feedwater Conference p8 Oct. 1970.
  33. EFFERTZ P.H. FICHTE W. SZENKER B RESCH G. BURGMANN F. GRUNSLAGER E. and BEETZ E. VGB Kraftwerkstechnik 58, 585, 1978.
  34. HOMIG H.E. Mitt V.G.B., 76, 12, 1962.
  35. BOHNSACK G. V.G.B. Feedwater Conference, p.2, 1971
  36. BORSIG F. Der Maschinenschaden, 41, 3, 1968.
  37. ASHFORD J.H. BIGNOLD G.J. DE WHALLEY C.H. FINNIGAN D.J. GARBETT K MANN G.M.W. MCFALL F. and WOOLSEY I.S. CEGB Report RD/L/N 126/79.
  38. CONLON T.W. WEAR 29, 69, 1974.
  39. FINNIGAN D.P. GARBETT K and WOOLSEY I.S. to be reported.
  40. BERGER F.P. and HAU K. -F. F-L. Int J. Heat Mass Transfer, 20, 1185, 1977.
  41. TAGG D.J. PATRICK M.A. and WRAGG A.A. Trans. I. Chem.E. 57, 12, 1979.
  42. SWEETON F.H. and BAES C.F. J.Chem. Thermodynamics, 2, 479, 1970.
  43. CONEY M. Private Communication.